Available online at www.sciencedirect.com
ScienceDirect
MATTER AND RADIATION AT EXTREMES
Matter and Radiation at Extremes 1 (2016) 237−248
www.journals.elsevier.com/matter-and-radiation-at-extremes

Review article

Review of quantum collision dynamics in Debye plasmas

R.K. Janev [b], Songbin Zhang [a,*], Jianguo Wang [c]

[a] School of Physics and Information Technology, Shaanxi Normal University, Xi'an 710119, China
[b] Macedonian Academy of Sciences and Arts, P.O. Box 428, 1000 Skopje, Macedonia
[c] Key Laboratory of Computational Physics, Institute of Applied Physics and Computational Mathematics, P.O. Box 8009, Beijing 100088, China

Received 1 June 2016; revised 15 August 2016; accepted 16 August 2016
Available online 14 October 2016

Abstract

Hot, dense plasmas exhibit screened Coulomb interactions, resulting from the collective effects of correlated many-particle interactions. In the lowest particle correlation order (pair-wise correlations), the interaction between charged plasma particles reduces to the Debye−Hückel (Yukawa-type) potential, characterized by the Debye screening length. Due to the importance of Coulomb interaction screening in dense laboratory and astrophysical plasmas, hundreds of theoretical investigations have been carried out in the past few decades on the plasma screening effects on the electronic structure of atoms and their collision processes employing the Debye−Hückel screening model. The present article aims at providing a comprehensive review of the recent studies in atomic physics in Debye plasmas. Specifically, the work on atomic electronic structure, photon excitation and ionization, electron/positron impact excitation and ionization, and excitation, ionization and charge transfer of ion-atom/ion collisions will be reviewed.

PACS Codes: 32.80.-t; 32.70.-n; 34.70.-e; 34.80.-i; 52.20.-j

Keywords: Debye plasmas; Screened Coulomb potential; Atomic structure; Collision dynamics

1. Introduction

The study of Coulomb interaction screening in plasma environments is one of the major subjects in plasma physics [1−6]. The Coulomb interaction screening in plasma environments is a collective effect of correlated many-particle interactions [7−9]. It strongly affects the electronic structure (spectral) properties of atoms and properties of their collision processes with respect to those for isolated systems. Indeed, it has been observed experimentally in a number of laser-produced dense plasmas that the atomic spectral lines are significantly redshifted [10−14]. Note that the Debye−Hückel screening of Coulomb interaction between charged particles also appears in electrolytes, solid-state matter and many other physical systems (in nuclear physics it is known as Yukawa potential).

Extensive studies have been performed on the screening effects in classical hot, dense plasmas in the past decades (see examples in Refs. [7,8] and references therein). These studies have been motivated mainly by the researches in laser-produced plasmas, extreme ultraviolet (EUV) and X-ray laser developments, inertial confinement fusion and astrophysics (stellar atmospheres and interiors). The densities (n) and temperatures (T) in these plasmas span the ranges $n \sim 10^{15}-10^{18}$ cm^{-3}, $T \sim 0.5-5$ eV for stellar atmospheres, $n \sim 10^{19}-10^{21}$ cm^{-3}, $T \sim 50-300$ eV for laser-produced plasmas and $n \sim 10^{22}-10^{26}$ cm^{-3}, $T \sim 0.5-10$ keV for inertial confinement fusion plasmas. In classical hot, dense plasmas, both Coulomb and thermal effects play important roles. The

* Corresponding author.
E-mail address: song-bin.zhang@snnu.edu.cn (S.B. Zhang).
Peer review under responsibility of Science and Technology Information Center, China Academy of Engineering Physics.

http://dx.doi.org/10.1016/j.mre.2016.10.002

relative importance of these two effects can be estimated by the so-called coupling parameter $\Gamma = \frac{\langle Z_i e\rangle^2}{R_i k_B T_e}$, where $\langle Z_i e\rangle$ is the average charge of ions in the plasma, $R_i = \left(\frac{3}{4\pi n_e}\right)^{1/3}$ is the average inter-ionic distance, k_B is the Boltzmann constant, T_e and n_e are the plasma electron temperature and density, respectively [4]. In the weakly coupled plasmas with relatively high temperatures and low densities, such as those created by laser irradiation of solids and existed in the inertial confinement fusion or the stellar interiors, the potential energy is relatively small compared to the kinetic energy, and long-range self-consistent interactions (described by the Poisson equation) dominate over short-range two-particle interactions (collisions) where $\Gamma \ll 1$. To the lowest particle correlation order (pair-wise correlations), the complete screened Coulomb potential in a more general way is given by [5,6,15–18].

$$V(r) = \begin{cases} -Ze^2\left(\frac{1}{r} - \frac{1}{D+D_A}\right), & r \le D_A \\ -Ze^2\frac{D}{D+D_A}\frac{1}{r}\exp\left(-\frac{r-D_A}{D}\right), & r \ge D_A \end{cases}, \tag{1}$$

where Z is the nuclear charge, $D = \frac{(k_B T_e)^{1/2}}{(4\pi e^2 n_e)^{1/2}}$ and D_A are the screening length and the mean minimum radius of the ion sphere, respectively. D_A defines the ion sphere radius where the potential outside the ion sphere is screened by the plasmas, and $D_A < D$. In the limit when $D_A \to 0$, Eq. (1) reduces to the most often used Debye–Hückel (Yukawa-type) potential [7,8,19] as

$$V(r) = -\frac{Ze^2}{r}\exp\left(-\frac{r}{D}\right). \tag{2}$$

The Debye–Hückel representation of plasma-screened Coulomb interaction is appropriate for weakly coupled plasmas, $\Gamma \ll 1$, when the thermal effects dominate over the Coulomb ones. It is obvious from Eq. (2) that for $D \to \infty$, the Debye–Hückel potential approaches the Coulomb potential.

Alternatively, in strongly-coupled plasmas with relatively low temperature and high density ($\Gamma \ge 1$), the Coulomb effects are dominant (such as in the solid phase) and the ions are packed tightly together; each ion occupies an equal volume and is surrounded by a sphere of radius $R_Z = \left[\frac{3(Z-1)}{4\pi n_e}\right]^{1/3}$ (ion-sphere radius). Under these conditions, the plasma-screened Coulomb interaction is described by the ion sphere model potential, defined as [1,2,4,19].

$$V(r) = \begin{cases} -\frac{Ze^2}{r}\left[1 - \frac{r}{2R_Z}\left(3 - \frac{r^2}{R_Z^2}\right)\right], & r \le R_Z \\ 0, & r > R_Z \end{cases}. \tag{3}$$

Note that in the screened model Eq. (1) or Eq. (2), the thermal plasma effects dominate over the Coulomb effects, while in the potential Eq. (3) the opposite is true. Obviously they describe two different types of classical plasmas. Note that recently an analytical finite temperature ion sphere model was presented by Li et al. [20]. More information about the models of these plasmas can be found in Refs. [1,2,4,6,7,20]. It should be noted that recently a modified Debye–Hückel potential [21–24] has been proposed to describe the interaction screening in dense quantum plasmas, where the de Broglie wavelength of the charge carriers is comparable to or larger than the inter-particle distance and the plasma temperature is smaller than the Fermi temperature. Shukla and Eliasson [23] have shown that the effective potential of a test charge in a dense quantum plasma has the form of an exponential-cosine screened Coulomb potential as

$$V(r) = -\frac{Ze^2}{r}\exp\left(-k_q r/\sqrt{2}\right)\cos\left(k_q r/\sqrt{2}\right), \tag{4}$$

where $k_q = \left(\frac{4m^2\omega_p^2}{\hbar^2}\right)^{1/4}$ is the electron quantum wave number, m is the electron mass, and $\omega_p = \sqrt{4\pi n e^2/m}$ is the electron plasma frequency. Usually quantum plasmas are characterized by a very low temperature and a high number density. Such plasmas exist in metals, semiconductor devices, nanoscale structures (nanowires, quantum dots) and compact astrophysical objects (neutron stars, white dwarfs).

The above model potentials describe the interactions between the electron and the charged ion, while there are different arguments about whether a similar Coulomb screening between two atomic electrons should be applied [1,4,15]. Generally, three types of models are employed in Debye plasmas in this respect: The first one does not consider any screening [25],

$$V_{ee}(r_1, r_2) = \frac{e^2}{|\boldsymbol{r}_1 - \boldsymbol{r}_2|}, \tag{5}$$

where $\boldsymbol{r}_1$ and $\boldsymbol{r}_2$ are the electron coordinates. The second one considers only the screening on one electron coordinate [4],

$$V_{ee}(r_1, r_2) = \frac{e^2}{|\boldsymbol{r}_1 - \boldsymbol{r}_2|}\exp\left(-\frac{|\boldsymbol{r}_1|}{D}\right). \tag{6}$$

The third one considers the screening on both coordinates [1],

$$V_{ee}(r_1, r_2) = \frac{e^2}{|\boldsymbol{r}_1 - \boldsymbol{r}_2|}\exp\left(-\frac{|\boldsymbol{r}_1 - \boldsymbol{r}_2|}{D}\right). \tag{7}$$

In most of the recent works the last type of models is taken.

In the present review, we provide a comprehensive overview of the fundamental theoretical studies of atomic physics in Debye plasmas modeled with screened interactions (Eq. (2) and Eq. (7)) in the past decade; earlier comprehensive reviews of hot-dense plasmas can be found in Refs. [1,6–8]. In the sections below we summarize the work on atomic structure, photon collisions, electron collisions, positron collisions, and heavy particle collisions in a wide range of plasma screening conditions. Atomic units will be used in the remaining part of this article, unless explicitly indicated.

2. Atomic structure

In the nonrelativistic approximation, the radial Schrödinger equation for the hydrogenlike ion with nuclear charge Z in screened potential (Eq. (2)), under the scaling transformations $\rho = Zr$, $\delta = ZD$, takes the form of that for the hydrogen atom as

$$\left[-\frac{d^2}{2d\rho^2}+\frac{l(l+1)}{2\rho^2}-\frac{\exp(-\rho/\delta)}{\rho}\right]P_{nl}(\rho,\delta)=\varepsilon_{nl}(\delta)P_{nl}(\rho,\delta), \tag{8}$$

where $\varepsilon_{nl}(\delta) = E_{nl}/Z^2$ and $P_{nl}(\rho,\delta)$ are the scaled energy and wave function, respectively. Thus, the results (energy levels, wave functions, photoionization cross sections) obtained for the hydrogen atom can be scaled to higher Z. The most prominent feature of the screened potential Eq. (2) is the lifting of the Coulomb l-degeneracy of the energy levels of hydrogenlike system (i.e., the energy of hydrogenic level n splits into n components). Another important feature of the potential Eq. (2) is that for any finite δ, it supports only a finite number of bound nl states [17,18]. This implies that with decreasing δ, the binding energies of nl states decrease and the nl energy levels successively enter the continuum at certain critical screening lengths δ_{nl}, obeying the relations of $\delta_{n+1,l} > \delta_{nl}$ and $\delta_{n,l+1} > \delta_{nl}$. Table 1 shows the scaled critical screening lengths of hydrogenlike ions for the states with $n \le 6$ [26]. Furthermore, with decreasing δ, the excitation threshold energies also decrease. For a given n, the states with lower l value have lower thresholds for any fixed value of δ. As a consequence of the decrease of bound state energies when δ decreases, the corresponding wave functions become increasingly more diffuse [27].

For the hydrogenlike system with large nuclear charge Z, the relativistic effect becomes important. Fine structures of the energy levels and large and small components of the wave functions arise and should be studied with the Dirac equation [28]. By taking the transformations of $\rho = Zr$ and $\delta = ZD$, the radial wave functions of Dirac equation with the screened potential Eq. (2) is reduced to the scaled form as

$$\begin{pmatrix} -\frac{\exp(-\rho/\delta)}{\rho}-\varepsilon_{gk}(\xi,\delta) & \frac{1}{\xi}\left(\frac{k}{\rho}-\frac{d}{d\rho}\right) \\ \frac{1}{\xi}\left(\frac{k}{\rho}+\frac{d}{d\rho}\right) & -\frac{\exp(-\rho/\delta)}{\rho}-\frac{2}{\xi^2}-\varepsilon_{gk}(\xi,\delta) \end{pmatrix} \times \begin{pmatrix} P_{gk}(\delta,\rho) \\ Q_{gk}(\delta,\rho) \end{pmatrix} = 0, \tag{9}$$

Table 1
Values of the critical scaled screening length of hydrogenlike ions for the states with $n \le 6$ [26].

n	l					
	0	1	2	3	4	5
1	0.839907					
2	3.222559	4.540956				
3	7.171737	8.872221	10.947492			
4	12.686441	14.730720	17.210209	20.067784		
5	19.770154	22.130652	24.984803	28.257063	31.904492	
6	28.427266	31.080167	34.285790	37.949735	42.018401	46.458584

where $\xi = Z/c$, $k = \pm(j+1/2)$ for $l = j\pm1/2$ is the relativistic momentum quantum number, $\varepsilon_{gk}(\xi,\delta)$ is the scaled energy. For bound states $g = n$, with n being the principal quantum number, and for continuum states $g = \varepsilon$, with ε being the kinetic energy of continuum electron. $P_{gk}(\delta,\rho)$ and $Q_{gk}(\delta,\rho)$ are the scaled large and small components of the electron wave function, whose scaled factors for the bound or continuum states are different. Eq. (9) also indicates that in contrast to the nonrelativistic case, the results for $Z = 1$ states cannot be scaled to any higher Z [29,30]. Fig. 1 shows the scaled energies of $1s_{1/2}$, $2s_{1/2}$, $2p_{1/2;3/2}$, $3s_{1/2}$, $3p_{1/2;3/2}$ and $3d_{3/2;5/2}$ states of Fe^{25+} as functions of δ, investigated by Xie et al. [29] As shown in Fig. 1(a), the energy splitting of nl states increases with decreasing δ, while the relativistic fine structure energy splitting of nl-states (noticeable in Fig. 1 for large values of δ) decreases with decreasing δ. Fig. 1(b) illustrates that with increased δ, the scaled relativistic binding energies increase with increased Z and that the fine structure component of the nl manifold with larger j-value has a smaller binding energy than the one with smaller j. The scaled critical screening lengths, δ_{nlj}, at which the binding energy of nlj state becomes zero, are 0.8343, 3.2048, 4.5047 and 4.5342 a.u. for $1s_{1/2}$, $2s_{1/2}$, $2p_{1/2}$ and $2p_{3/2}$ states, respectively. More information of the screening effects on the wave functions and phases of the continuum states can be found in the work of Xie et al. [29].

For the three-body systems in Debye plasmas, significant attention has been paid to the screening effects on the resonant states (such as doubly excited states in two electron atomic systems or resonances in electron-atom scattering). These states play very important roles in the threshold electron dynamics, resulting in the drastic changes of the threshold photoionization [31], electron-impact excitation [32–34] and ionization [35,36]. Ho and his associates have performed systematic and comprehensive investigations of doubly excited states or resonances of the typical three-body systems with the screening potentials, such as the hydrogen negative ion (H^-) [37–41], the positronium negative ion (Ps^-) [42–46], helium [47–49] and helium-like ions [50,51]. We note that for many-electron atomic systems (with more than two electrons), most of the earlier works have incorporated the Debye screenings only in the electron-nucleus potential of Eq. (2) and Eq. (5), owing to the complicated derivation of the two-body screening potential and difficulties to perform the calculations [52]. But the screening effects on the valence electron dynamics of Li and Na are efficiently studied based on the model potential formalism [53–58].

The plasma screening effects on the polarizability is another active topic, since the polarizability is an important characteristic of an atomic or molecular system describing its response to an external electric field. Qi et al. [59] systematically studied the static dipole polarizability of hydrogenlike ions in Debye plasmas. They found that with decreasing δ, the contribution of the bound states to the polarizability decreases and that of continuum states increases. As a result, both the polarizabilities of 1s and 2s states gradually increase when δ decreases to the critical screening length at which the 2p

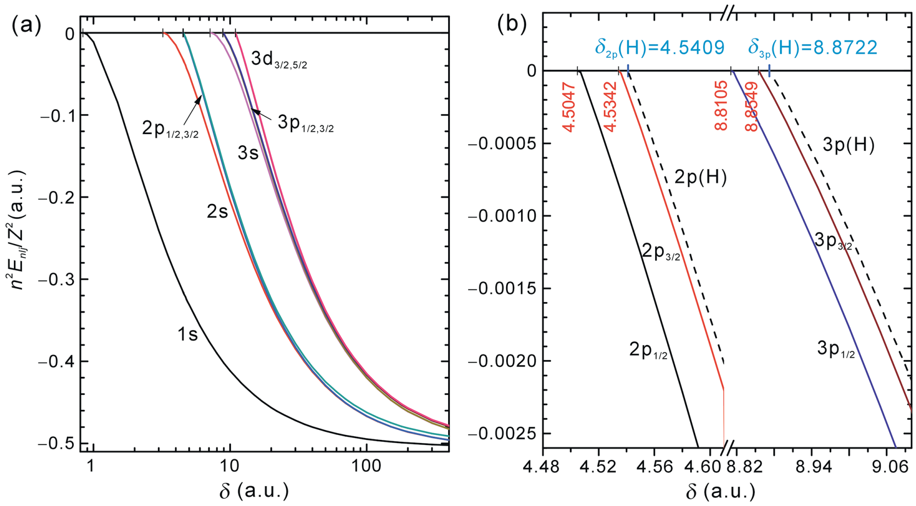

Fig. 1. (a) Scaled energies of 1s, $2l_j$ and $3l_j$ states of Fe^{25+} ($Z = 26$) ion as functions of scaled screening length, and (b) behavior of $2p_{1/2}$, $2p_{3/2}$, $3p_{1/2}$ and $3p_{3/2}$ energies near the critical screening lengths δ^c_{nlj} for Fe^{25+} (solid lines) and for hydrogen atom ($Z = 1$) (dashed lines) [29].

state merges into continuum, followed by a drastic increase when 1s and 2s states become continuum states, respectively, and after that only the continuum states contribute to the polarizability. Note that Ho and his associates have also studied the screening effects on the polarizabilities of hydrogen atom, H^-, He and He-like ions [60−62]. Polarizabilities of Li and Na in Debye plasmas are also broadly investigated based on the model potential formalism [53,56−58,63,64].

Spectroscopy is the most direct approach to study the screening effects on the atomic structure. Margenau et al. [6] and Sil et al. [65] have reviewed the spectroscopy in plasmas. Recently, the redshifts of atomic spectral lines have also been observed experimentally in a number of laser-produced dense plasmas [10−14]. Although there are many new relevant works [66−71], it is interesting to mention the work of Chang et al. [71] When simulating the redshift of the Lyman-α emission line of H-like ions in plasmas, the calculations with a judicial choice of the radius of Debye sphere of the general Debye potential Eq. (1) generated the results which are in good agreement with the experimentally observed values, in addition reproduced the simulated data in consistent with more elaborate simulations based on quantum mechanical approaches.

3. Photon collisions

Studies of photo-excitation process in plasmas are mainly concentrated on the calculations of oscillator strengths [60,70,72−79], since the photo-excitation cross sections and radiative transition probabilities are directly related to the oscillator strengths [80]. Qi et al. [70,74] gave a systematic presentation of the scaled spectral properties of hydrogenlike ions in Debye plasmas, including the transition frequencies, absorption oscillator strengths, and radiative transition probabilities. The line intensities of the Lyman and Balmer series are also presented in these references for a wide range of plasma screening parameters. It is shown that for $\Delta n \neq 0$ transitions, the oscillator strengths and spectral line intensities decrease with increased plasma screening, while those for $\Delta n = 0$ transitions rapidly increase. The lines associated with $\Delta n \neq 0$ transitions are redshifted, whereas those for $\Delta n = 0$ transitions are blueshifted [70].

The plasma effects on the photoionization process have been studied in the past under various assumptions about the form of screening defined by the plasma conditions [7,8]. Studies of this process in a Debye plasma were reported in many papers [15,26,29,31,54,55,72,73,81−90]. The most prominent screening effects of the Debye plasmas on the energy behavior of photoionization cross sections of hydrogenlike ions are manifested in its low-energy region, i.e. Wigner threshold law, an appearance of multiple shape and virtual-state resonances when the photoelectron energy is close to the bound or continuum energy of nl states in the vicinity of their critical screening length, an appearance of multiple Cooper minima associated with n, $l + 1$ shape resonances, a (slight) reduction of the cross section at high photoelectron energies [26]. As shown in Fig. 2 [29], when δ decreases to some critical values, the total scaled photoionization cross sections from the ground state of hydrogen atom and Fe^{25+} ion in Debye plasmas are dominated by the contributions from shape resonances. Since relativistic effect is very important for Fe^{25+} ion, the energy behavior and the magnitude of the scaled cross sections with the same δ for H and Fe^{25+} behave differently. They are identical for the unscreened case, very close for $\delta = 20$, 9 and 5 a.u., but quite different for other selected δ. All observed differences and similarities between the cross sections in the figure for the same δ can be easily understood by taking into account the difference in the fine-structure energy splitting of bound states between H and Fe^{25+} ions and that all other considered values of δ lie in the vicinity of critical screening lengths at which $2p_{1/2;3/2}$ and $3p_{1/2;3/2}$ states merge into the continuums. Two or one resonance peaks appear in the photoionization of Fe^{25+}

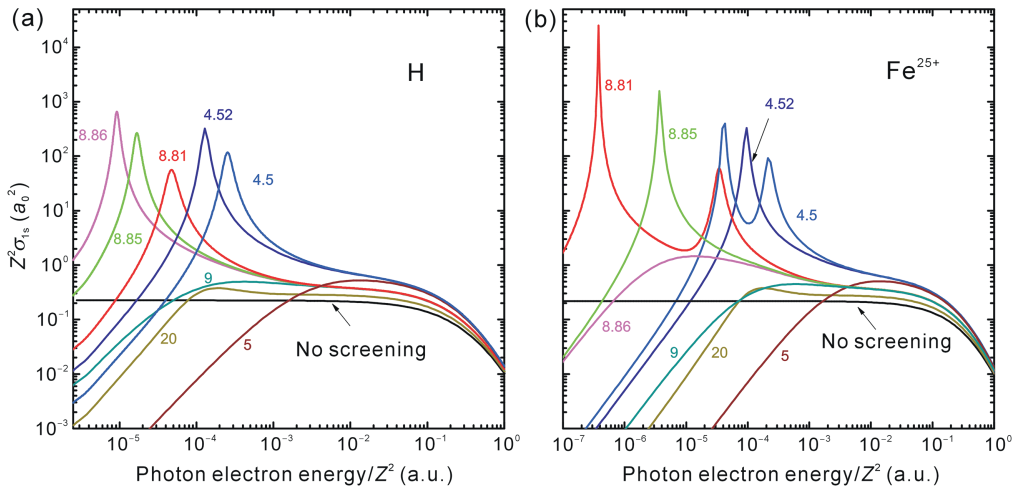

Fig. 2. Scaled total photoionization cross sections for the ground $1s_{1/2}$ state of (a) hydrogen ($Z = 1$) atom and (b) Fe^{25+} ($Z = 26$) ion as functions of scaled photoelectron energy for different scaled screening lengths [29].

for a given screening length depending on whether a shape resonance is formed in both $1s_{1/2}\rightarrow \varepsilon p_{1/2}$ and $1s_{1/2}\rightarrow \varepsilon p_{3/2}$ transitions or only in one of them. Note that in the case of H atom where the fine-structure splitting is negligible, the critical screening lengths of $p_{1/2}$ and $p_{3/2}$ states coincide and so do the shape resonances ($p_{1/2;3/2}$), producing only one resonance peak in photoionization cross sections.

In many electron atomic systems, Feshbach resonances [91] dominate the photoionization cross sections in the low energy region. In such cases, the screening effects alter the properties of the resonances, resulting in the significant changes in the cross sections [15,31,89]. A typical example is the photodetachment of hydrogen negative ions in Debye plasmas [31], where the transformation of a Feshbach resonance into a shape resonance happens with the decrease of screening length, as shown in Fig. 3. Such transformation is manifested in the photoionization cross sections as the shape of the contributed peak changes from “asymmetric” to “symmetric”. A more detailed description of the crossover of Feshbach resonances to shape resonances is given in the next section and in Refs. [33,34]. Due to the softening of the screening potentials, the positions of the peaks or the resonances shift to the lower energies.

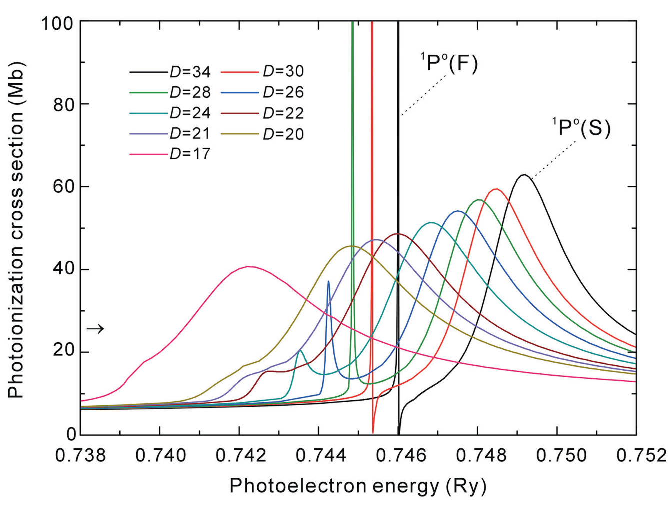

Fig. 3. Dynamic evolution of photodetachment cross sections around $n = 2$ excitation threshold for different screening lengths [31]. $^1P^o(T)$ denotes the dominant resonance, where T = F (Feshbach) or S (Shape) resonances.

Another remarkable feature of the screening effects on the photoionization cross sections is the appearance of Cooper minima [92,93]. No Cooper minima exist in the photoionization cross sections from 2s or 3s states of hydrogenlike ion and ground state of Li atom in the unscreened case. However, Cooper minima can appear in both of these two cases when the screening interactions increase to some extent [26,54,55,84,86,87]. In the hydrogenlike ion in Debye plasmas, Cooper minima do not appear from the states whose radial wave functions do not have nodes, but Combet-Farnoux minima [94] are observed from these states [26].

4. Electron collisions

In 1980s, Weisheit et al. [1,4,95] studied the plasma screening effects on electron-impact excitation and ionization of hydrogenlike ions by the first Born approximation and close-coupling methods. In the studies, the screening interaction between the projectile electron and target electron was considered, but the changes of target wave functions and bound state energies were not taken into account. Schlanges and Bornath [96,97] calculated the electron impact ionization and three body recombination coefficients for a dense nonideal hydrogen plasma by the first Born approximation. Later, Jung et al. [98–102] have also investigated the plasma screening effects on electron-impact excitation and ionization processes in the Born approximation and the semiclassical impact parameter approximation, in which the plasma screening effects on both the bound and scattering electrons were considered. The variational method combined with the perturbation theory was applied to calculate the target bound states in the screened potential. These studies found that the plasma screened interaction significantly alters the electron-impact excitation/ionization cross sections.

It is well known that resonances play very important roles in electron-atom scattering and dominate the excitation cross sections in low energy region, especially the near-threshold region. Zhang et al. [32–34] were the first to address the effects of screened Debye–Hückel interaction on the electron-atom scattering and excitation in the energy region near the excitation threshold. The phenomenon of crossover of Feshbach resonances into shape-type resonances when the strength of the interaction screening varies was discovered. The electron-impact excitation of hydrogen atoms in the energy region near $n = 2$ and $n = 3$ excitation thresholds was investigated. The electron-proton and electron–electron screened Coulomb interactions were taken in the Debye–Hückel form (Eq. (2) and (7), respectively) and the R-matrix method with pseudo states [103,104] was used in scattering calculations. It was found that as the interaction screening increases, the $^{1;3}$P and ^{1}D Feshbach resonances transform into shape-type resonances when they pass across the 2s and 2p thresholds, respectively. As shown in Fig. 4, the widths of Feshbach resonances $^{1;3}$S, converging to the 2s threshold, rapidly decrease when the resonance approaches the threshold before it merges with the parent 2s state; while the widths of ^{1,3}P Feshbach resonances also considerably decrease when they approach the 2s threshold, but after passing it, their widths start to increase rapidly, which is a signature of the shape resonance (see the D dependence of ^{1}P^{o}(2) shape resonance in Fig. 4). It is argued that this phenomenon results from the lifts of the l degeneracy of $n = 2$ energy level by the screening interaction, and the changes of the main configurations of Feshbach resonances by the mixing of 2p state with higher l states. The resonance transformation leads to drastic effects in the 1s→1s, 1s→2s and 1s→2p excitation collision strengths in the $n = 2$ threshold collision energy region, as shown in Fig. 5 where the dynamic evolution of 1s→2s collision strengths when the screening length varies is displayed. When the ^{3}P^{o}(2) and ^{1}P^{o}(1) resonances have already acquired a shape-type character, peaks are clearly observed in

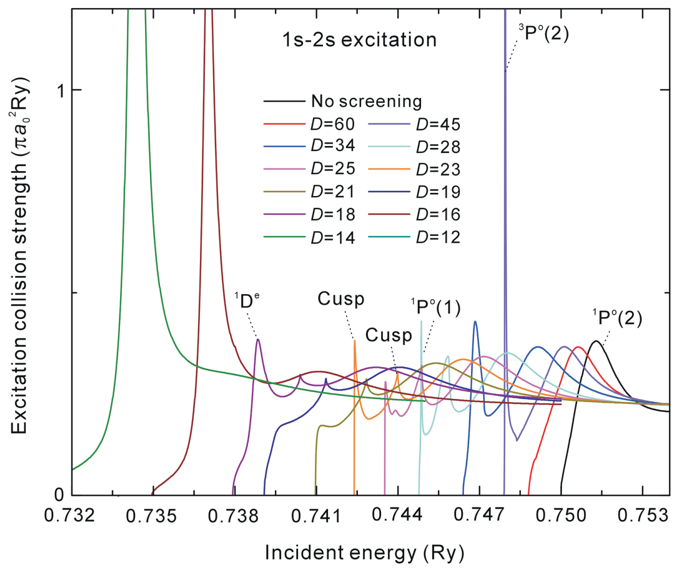

Fig. 5. Dynamic evolution of 1s→2s collision strength with decreased Debye length [33,34]. $^{2s+1}L^{\pi}(n)$ denotes the dominant resonance.

the 1s→2s collision strength for $D = 45$ a.u. (at $E = 0.74794$ Ry) and for $D = 29$ a.u. (at $E = 0.745118$ Ry), respectively. The effect of ^{1}D^{e} resonance on the 1s→2s collision strength is also observed after passing through the 2s threshold at $D = 19$ a.u. [33,34]. Similar phenomena are also observed near the $n = 3$ threshold, but the situation is more complex, since the threshold energy in the screened case splits into three components, with 3s, 3p, 3d energy levels having their own critical screening lengths [29]. Note that Kar and Ho [37–39,46] have systematically studied the resonances in hydrogen negative ion with screened Coulomb interaction employing the highly accurate complex-coordinate rotation and the stabilization methods.

For high energy electron scatterings, the fast projectile electron is hardly affected by the (screened) interaction potentials, and can be well described by a plane wave, and the excitation cross sections are directly related to the generalized oscillator strengths (GOS). However, the screened Coulomb interaction alters the bound state wavefunctions, resulting in the changes of GOS and excitation cross sections. Qi et al. [74] found that the plasma screening of the interaction reduces the GOS for transitions between the states with different n and increases the GOS between the states with the same n. The differential and total excitation cross sections are affected in a similar way when the strength of interaction screening varies.

Zammit et al. [105–107] performed comprehensive studies on the excitation and ionization processes in electron-hydrogen and electron-helium collisions in Debye plasmas employing the convergent close-coupling method [108] in the energy region from the threshold to several hundreds of eV. They found that as the strength of the screening increases, the excitation cross sections decrease, while the total ionization cross section increases.

Qi et al. [35,36] also studied the fast-electron-impact ionization process of hydrogen-like ions in Debye plasmas.

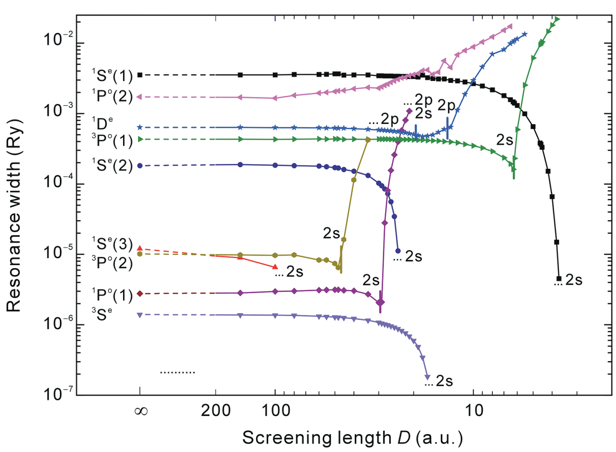

Fig. 4. Variation of the widths of Feshbach and shape resonances when the screening length decreases [33,34]. Short dashed lines represent the critical values of D where Feshbach resonances pass across 2s or 2p threshold.

They considered the single differential ionization cross sections (SDCS) of hydrogen-like ions in their 2s and 2p initial states and focused on the low energy spectrum of ejected electrons. The SDCS of 2p state is at an impact electron energy of 1 keV/Z^2 shown in Fig. 6 for a number of scaled screening length $\delta = ZD$ as a function of the scaled energy of ejected electrons. The appearance of the sharp peaks in the SDCS for $\delta = 10.88$, 10.90, 10.22 a.u. is related to the fact that for these values of δ, and the 3d electron bound state is already in the continuum ($\delta_{3d} = 10.947$ a.u., see Table 1) and the continuum εd electron is temporarily trapped by the centrifugal barrier of the effective potential, thus the ionization proceeds via the shape resonances in the effective potential (note that for $\delta = 11.0 > \delta_{3d}$ such peak is absent in the 2p SDCS). The SDCSs for $\delta = 7.21$ a.u. and 7.22 a.u. show an enhancement over a broader energy range of ejected electrons. These two values of δ are in the immediate vicinity of the critical screening length of 3s bound state ($\delta_{3s} = 7.172$ a.u.), indicating that the ionization process involves virtual intermediate states since for the s-continuum states there is no centrifugal barrier in the effective potential. The SDCSs for $\delta = 8.85$ a.u. and 8.89 a.u. show respectively a sharp peak and a broad enhancement in the low-energy region which are on the left and right side of the critical screening length of 3p state bound ($\delta_{3p} = 8.872$ a.u., cf. Table 1). The profiles for SDCS of fast-electron-impact ionization are similar to those of the photoionization cross sections of hydrogen-like ions in Debye plasmas [26,90], except that the photoionization process involves only dipole transitions while the electron-impact ionization sums over all multi-pole transitions.

5. Positron collisions

Collision processes involving positrons are of fundamental importance in various fields of physics [109], astrophysics [110—112] and also plasma physics [113—115]. Existence of positron in these plasma environments exhibits the importance

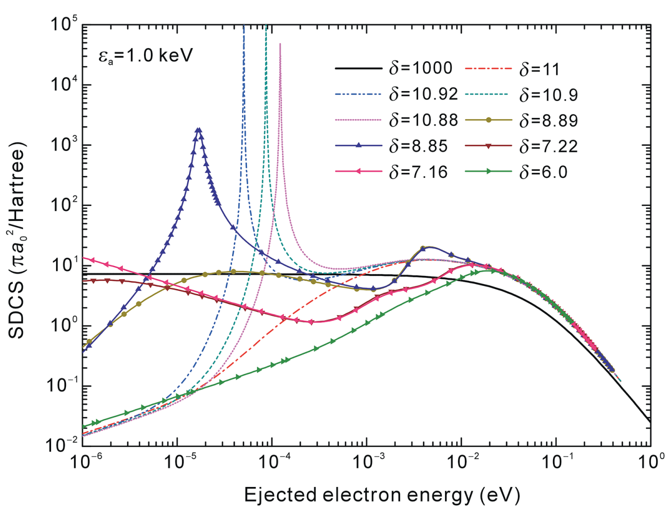

Fig. 6. Electron-impact single differential cross sections from 2p state of hydrogenlike ion with incident scaled energy $\varepsilon_a = 1$ keV [36].

of the study of positron-collision processes in plasma environment. Zhang et al. [116] studied positron-impact excitation of hydrogen atoms in Debye plasmas by using the close-coupling method without inclusion of the positronium formation channels. They found that the interaction screening decreases the coupling matrix elements, resulting in the significant reduction of excitation cross sections for 1s→2s, 1s→2p and 2s→2p transitions. This finding was supported by a more sophisticated treatment of Ghoshal et al. [117,118] employing the distorted-wave theory in the momentum space with inclusion of the positronium formation channels. Furthermore, the differential cross sections for the H(ns) →H(nl) elastic and inelastic transitions in both Debye and quantum plasmas have also been investigated by Ghoshal et al. [117—121].

Positronium (Ps) formation in positron-hydrogen atom collisions in Debye plasmas is another active topic [121—124]. Sen et al. [124] were the first to report positronium formation cross sections for positron-hydrogen atom collisions in Debye plasmas by using the second-order distorted-wave approximation. Later, Ma et al. [123] published Ps ($n = 1$, 2) formation cross sections obtained by employing the momentum-space coupled-channel optical method [125]. As shown in Fig. 7 the Ps formation threshold energy decreases as the values of D decreases, since the binding energy of the atomic electron decreases as the Debye length decreases. The Ps formation cross sections are significantly larger (particularly in the threshold region) than that in the plasma free case. It can be observed from the figure that when the screening length decreases, the position of the maximum of Ps formation cross section shifts towards lower energies while the magnitude of the cross section maximum increases. It can also be observed in this figure that the plasma screening effect on the Ps formation cross section decreases as the projectile energy increases [123,124]. We mention that Ghoshal et al. [121,122] also studied the plasma screening effects on the differential cross sections of Ps formation in positron-hydrogen atom collisions, while Pamdey et al. [126] studied the Ps formation in positron-alkali-metal collisions in Debye plasmas based on the Debye screening of an electron-ion core model potential.

6. Heavy particle collisions

The early studies involving heavy-particle collisions in hot, dense plasmas are those for proton-impact excitation of $n = 2$ fine structure levels of hydrogen-like ions within a close-coupling scheme employing both the static Debye—Hückel and the ion-sphere model potentials [2], the electron capture in proton-hydrogenic ion collisions [127] and the symmetry of the resonant charge exchange in hydrogen-like ion-parent nucleus collisions [128] by the classical Bohr-Lindhard model, and the classical trajectory Monte Carlo study of electron capture and ionization in hydrogen atom-fully stripped ion collisions [129]. However in those studies, the changes of the electronic structures (wave functions and energy levels) in the screened potential were taken into account at most within the first-order perturbation theory. Until recently, Wang and his

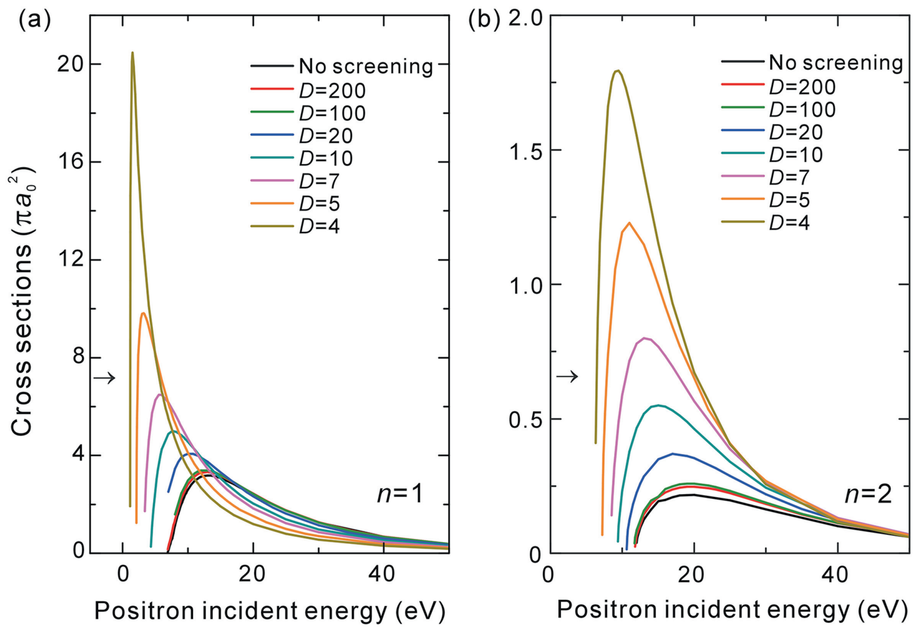

Fig. 7. (a) $n = 1$ and (b) $n = 2$ positronium formation cross sections in positron-hydrogen collisions for various Debye lengths [123].

associates performed nonperturbative comprehensive studies of the excitation, electron capture and ionization processes in Debye plasmas for H^{+}+H [130,131], He^{2+}+H [132,133], He^{2+}+He^{+} [134], C^{6+}+H [135], O^{6+}+H [136], N^{5+}+H [137] and O^{8+}+H [138] collision systems by using the two-center atomic orbital close-coupling (TC-AOCC) method [139] in the intermediate energy region (1−300 keV/u), and in H^{+}+H [140] and He^{+}+H [141] collisions by using the quantum-mechanical molecular orbital close-coupling (QMOCC) method [142] in the low energy region (<1 keV/u).

In the intermediate energy region, one typical work is the study of ionization in He^{2+}+H collisions [132] by the TC-AOCC method. Fig. 8 shows the ionization cross sections to the target continuum (ITC) and to the projectile continuum (IPC) for different screening lengths in the energy range of 5−300 keV/u [132]. With decreased D, the ITC cross section firstly increases in the entire energy range up to $D \leq 4$ a.u., then starts to decrease in the energy region above ~40 keV/u. This behavior can be attributed to the similar behavior of the direct coupling matrix elements. The IPC cross sections for the selected screening lengths have significant values only for energies below ~60 keV/u, and increase sharply with decreasing D. It can be understood from the fact that more and more bound states of He^{+} become continuum states with

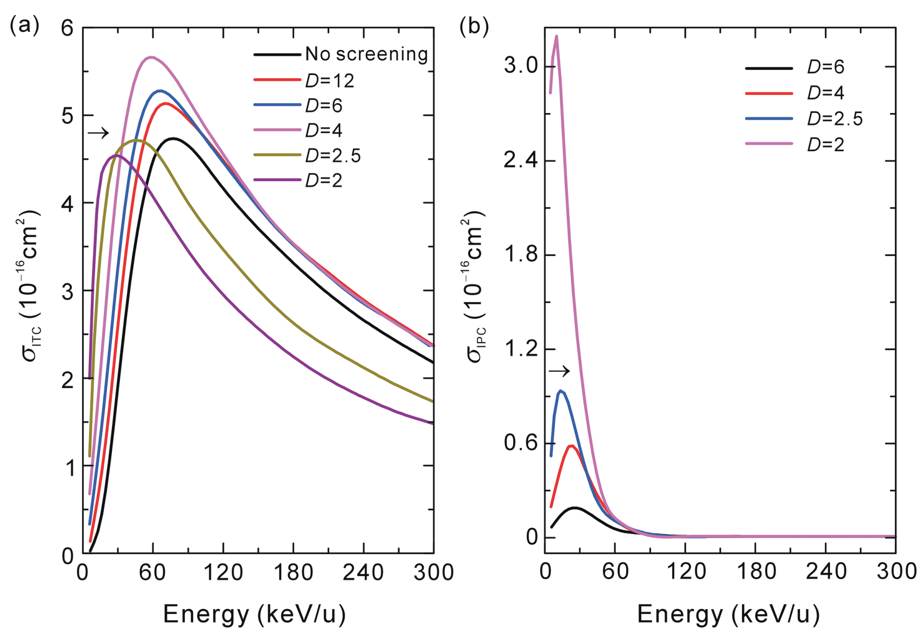

Fig. 8. Ionization cross sections to (a) target continuum (ITC) states and (b) projectile continuum (IPC) states for different Debye lengths [132].

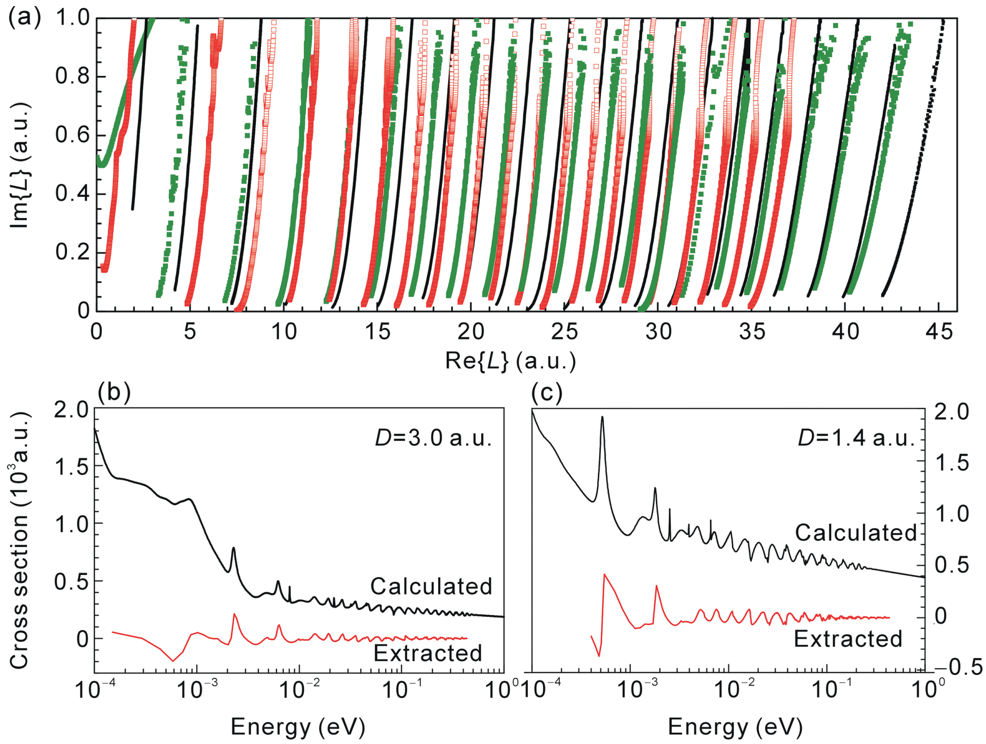

Fig. 9. Regge cross section calculation for H^{+}+H collision in Debye plasma with $D = 3.0$ and 1.4 a.u. [140]. (a) Regge trajectories in the energy range of 0.00006 eV $\leq E < 1$ eV for $D = \infty$ (black solid line), $D = 3.0$ a.u. (filled symbols) and $D = 1.4$ a.u. (hollow symbols). Extracted Regge contribution and exact quantal charge transfer cross sections for (b) $D = 3.0$ a.u. and (c) $D = 1.4$ a.u., respectively.

decreasing D, and when $D = 2$ a.u., the 2p(He^{+}) state, quasiresonantly coupled with the initial state 1s(H), also becomes a quasicontinuum state, leading to a drastic increase of the IPC cross section with respect to the case of $D = 2.5$ a.u..

It has been demonstrated in Ref. [129] that in H^{+}+H collisions the Regge poles of the scattering matrix are the physical origin of the oscillation structures in the elastic and electron capture cross sections in this collision system in the energy range of 0.01–1.0 eV. Wu et al. [140] recently studied the H^{+}+H collision in Debye plasma and calculated the scattering matrix by using the QMOCC method. As shown in Fig. 9, they found that the number of Regge oscillations in the elastic and resonant charge transfer cross sections is quasi-conserved when the plasma Debye length D is larger than 1.4 a.u., reflecting the invariance of the number of vibrational states of H_2^{+} with changing D in that region. Similarly, the frequency and amplitudes of glory oscillations in the elastic cross sections are quasi-invariant with the variation of D.

Note that in the high energy region, Pandey et al. [143,144] studied the charge exchange and ionizaiton in O^{8+}+H and He-like system+H collisions in Debye plasmas by classical trajectory Monte Carlo method, and Bhattacharya et al. [145] investigated the proton-hydrogen collisions in Debye plasmas by distorted wave formalism.

7. Summary

In conclusion, we reviewed the recent studies of the screening effects of Debye plasmas on the atomic structure and collision processes. The plasma screening effects affect the atomic structure in several fundamental ways: reducing the number of bound states, decreasing the energy of bound states, broadening the radial distributions of the bound states and changing the phase and amplitude of the continuum waves. All these changes drastically affect the dynamics of collision processes taking place in Debye plasmas. The studies of the electronic structure of atoms and their collision processes in Debye plasmas in past few decades have revealed many new features of the screening effects on atomic physics and have contributed to a better understanding of the properties of these plasmas. The newly acquired knowledge should be useful in the simulation and diagnostics of hot, dense plasmas.

Acknowledgment

Thanks to L.Y. Xie (Figs. 1 and 2), Y.Y. Qi (Fig. 6), J. Ma (Fig. 7), L. Liu (Fig. 8) and Y. Wu (Fig. 9) for sending us the ASCII data of their published papers. S.B. Zhang was supported by the starting grants of Shaanxi Normal University and the Organization Department of CCCPC. J.G. Wang was supported by the National Basic Research Program of China (Grant No. 2013CB922200).

References

[1] J.C. Weisheit, Atomic excitation in dense plasmas, Adv. At. Mol. Phys. 25 (1989) 101.

[2] K. Scheibner, J.C. Weisheit, N.F. Lane, Plasma screening effects on proton-impact excitation of positive ions, Phys. Rev. A 35 (1987) 1252.
[3] H. Nguyen, M. Koenig, D. Benredjem, M. Caby, G. Coulaud, Atomic structure and polarization line shift in dense and hot plasmas, Phys. Rev. A 33 (1986) 1279.
[4] B.L. Whitten, N.F. Lane, J.C. Weisheit, Plasma-screening effects on electron-impact excitation of hydrogenic ions in dense plasmas, Phys. Rev. A 29 (1984) 945.
[5] C.A. Rouse, Finite electronic partition function from screened Coulomb interactions, Phys. Rev. 163 (1967) 62.
[6] H. Margenau, M. Lewis, Structure of spectral lines from plasmas, Rev. Mod. Phys. 31 (1959) 569.
[7] D. Salzmann, Atomic Physics in Hot Plasmas, Oxford University Press, Oxford, 1998.
[8] M.S. Murillo, J.C. Weisheit, Dense plasmas, screened interactions, and atomic ionization, Phys. Rep. 302 (1998) 1.
[9] J. Hansen, I. McDonald, Theory of Simple Fluids, Academic, London, 1986.
[10] A. Saemann, K. Eidmann, I.E. Golovkin, R.C. Mancini, E. Andersson, et al., Isochoric heating of solid aluminum by ultrashort laser pulses focused on a tamped target, Phys. Rev. Lett. 82 (1999) 4843.
[11] M. Nantel, G. Ma, S. Gu, C.Y. Côté, J. Itatani, et al., Pressure ionization and line merging in strongly coupled plasmas produced by 100-fs laser pulses, Phys. Rev. Lett. 80 (1998) 4442.
[12] Y. Leng, J. Goldhar, H.R. Griem, R.W. Lee, C vi Lyman line profiles from 10-ps KrF-laser-produced plasmas, Phys. Rev. E 52 (1995) 4328.
[13] N.C. Woolsey, B.A. Hammel, C.J. Keane, C.A. Back, J.C. Moreno, et al., Competing effects of collisional ionization and radiative cooling in inertially confined plasmas, Phys. Rev. E 57 (1998) 4650.
[14] M. Goto, R. Sakamoto, S. Morita, Experimental verification of complete LTE plasma formation in hydrogen pellet cloud, Plasma Phys. Control. Fusion 49 (2007) 1163.
[15] T.N. Chang, T.K. Fang, Atomic photoionization in a changing plasma environment, Phys. Rev. A 88 (2013) 023406.
[16] C.A. Rouse, Bull. Am. Phys. Soc. 9 (1964) 731.
[17] G. Ecker, W. Kröll, Lowering of the ionization energy for a plasma in thermodynamic equilibrium, Phys. Fluids 6 (1963) 62.
[18] G. Ecker, W. Weizel, Zustandssumme und effektive Ionisierungsspannung eines Atoms im Inneren des Plasmas, Ann. Phys. 452 (1956) 126.
[19] D.D. Clayton, Principles of Stellar Evolution and Nucleosynthesis, University of Chicago press, 1968.
[20] X. Li, F.B. Rosmej, Quantum-number-dependent energy level shifts of ions in dense plasmas: A generalized analytical approach, EPL 99 (2012) 33001.
[21] G. Hall, Ionized impurity scattering in semiconductors, J. Phys. Chem. Solids 23 (1962) 1147.
[22] V. Bonch-Bruevich, S.M. Kogan, The theory of electron plasma in semiconductors, Sov. Phys. Solid State 1 (1960) 1118.
[23] P.K. Shukla, B. Eliasson, Screening and wake potentials of a test charge in quantum plasmas, Phys. Lett. A 372 (2008) 2897.
[24] Y.Y. Qi, J.G. Wang, R.K. Janev, Bound-bound transitions in hydrogen-like ions in dense quantum plasmas, Phys. Plasmas 23 (2016) 073302.
[25] D. Ray, P.K. Mukherjee, Magnetic multipole transitions of a stripped carbon ion in a variety of Debye plasmas, J. Phys. B 31 (1998) 3479.
[26] Y.Y. Qi, J.G. Wang, R.K. Janev, Dynamics of photoionization of hydrogenlike ions in Debye plasmas, Phys. Rev. A 80 (2009) 063404.
[27] W. Kohn, C. Majumdar, Continuity between bound and unbound states in a Fermi gas, Phys. Rev. 138 (1965) A1617.
[28] I.P. Grant, Relativistic Quantum Theory of Atoms and Molecules: Theory and Computation, vol. 40, Springer Science & Business Media, 2007.
[29] L.Y. Xie, J.G. Wang, R.K. Janev, Relativistic effects in the photoionization of hydrogen-like ions with screened Coulomb interaction, Phys. Plasmas 21 (2014) 063304.
[30] D. Bielińska-Waż, J. Karwowski, B. Saha, P.K. Mukherjee, Relativistic effects in hydrogenlike atoms embedded in Debye plasmas, Phys. Rev. E 69 (2004) 016404.
[31] S.B. Zhang, J.G. Wang, R.K. Janev, Y.Z. Qu, X.J. Chen, Photodetachment of hydrogen negative ions with screened Coulomb interaction, Phys. Rev. A 81 (2010) 065402.
[32] S.B. Zhang, J.G. Wang, R.K. Janev, X.J. Chen, Electron-hydrogen atom-impact 1s → 2s and 1s → 2p excitation with screened Coulomb interaction between the n=2 and n=3 excitation thresholds, Phys. Rev. A 83 (2011) 032724.
[33] S.B. Zhang, J.G. Wang, R.K. Janev, Crossover of Feshbach resonances to shape-type resonances in electron-hydrogen atom excitation with a screened Coulomb interaction, Phys. Rev. Lett. 104 (2010) 023203.
[34] S.B. Zhang, J.G. Wang, R.K. Janev, Electron-hydrogen-atom elastic and inelastic scattering with screened Coulomb interaction around the n=2 excitation threshold, Phys. Rev. A 81 (2010) 032707.
[35] Y.Y. Qi, D.D. Ye, J.G. Wang, Y.Z. Qu, Fast-electron-impact ionization process by 3p of hydrogen-like ions in Debye plasmas, Chin. Phys. B 24 (2015) 033403.
[36] Y.Y. Qi, L.N. Ning, J.G. Wang, Y.Z. Qu, Plasma effect on fast-electron-impact-ionization from 2p state of hydrogen-like ions, Phys. Plasmas 20 (2013) 123301.
[37] L. Jiao, Y. Ho, Doubly excited P-wave resonance states of H^- in Debye plasmas, Phys. Plasmas 20 (2013) 083303.
[38] S. Kar, Y. Ho, Doubly excited $^{1,3}P^e$ resonance states of helium and the hydrogen negative ion interacting with Coulomb and screened Coulomb potentials, Phys. Rev. A 83 (2011) 042506.
[39] S. Kar, Y. Ho, Resonances in electron−hydrogen scattering in Debye plasmas, J. Phys. B 44 (2010) 015001.
[40] A. Ghoshal, Y. Ho, Ground states and doubly excited resonance states of H^- embedded in dense quantum plasmas, J. Phys. B 42 (2009) 175006.
[41] L. Jiao, Y. Ho, Doubly-excited $2p^2\ ^3P^e$ state of the hydrogen negative ion in Debye plasmas, J. Quant. Spectrosc. Radiat. Transf. 144 (2014) 27.
[42] A. Ghoshal, Y. Ho, Properties of the positronium negative ion interacting with exponential cosine-screened Coulomb potentials, Few-Body Syst. 46 (2009) 249.
[43] S. Kar, Y. Ho, D-wave resonances in three-body system Ps^- with pure Coulomb and screened Coulomb (Yukawa) potentials, Few-Body Syst. 45 (2009) 43.
[44] Y. Ho, S. Kar, Complex-scaling calculations for doubly excited resonances in Ps^- interacting with screened Coulomb (Yukawa) potentials, Few-Body Syst. 53 (2012) 437.
[45] Y. Ning, Z.C. Yan, Y.K. Ho, An investigation of resonances in e^+-H scattering embedded in Debye plasma, Phys. Plasmas 22 (2015) 013302.
[46] S. Kar, Y.K. Ho, Shape resonance in the Ps^- system, Phys. Rev. A 86 (2012) 014501.
[47] A. Ghoshal, Y. Ho, Doubly excited resonance states of helium in exponential cosine-screened Coulomb potentials, Phys. Rev. A 79 (2009) 062514.
[48] S. Kar, Y. Ho, Doubly excited nonautoionizing P, D, and F states of helium with Coulomb and screened Coulomb potentials, Phys. Rev. A 79 (2009) 062508.
[49] L.G. Jiao, Y.K. Ho, Complex-scaling calculations for resonance states of he with screened coulomb potentials, Int. J. Quantum Chem. 113 (2013) 2569.
[50] S. Kar, Y. Ho, Effect of screened Coulomb potentials on the resonance states of two-electron highly stripped atoms using the stabilization method, J. Phys. B 42 (2009) 044007.
[51] A. Ghoshal, Y.K. Ho, Doubly excited resonance states of two-electron systems in exponential cosine-screened Coulomb potentials, Comput. Phys. Commun. 182 (2011) 122.
[52] M. Das, B. Sahoo, S. Pal, Plasma-screening effects on the electronic structure of multiply charged Al ions using Debye and ionsphere models, arXiv:1604.01735, 2016.
[53] Y.Y. Qi, L.N. Ning, Dynamic processes and polarizability of sodium atom in Debye plasmas, Phys. Plasmas 21 (2014) 033301.
[54] Y.Y. Qi, Y. Wu, J.G. Wang, Photoionization of Li and radiative recombination of Li^+ in Debye plasmas, Phys. Plasmas 16 (2009) 033507.

[55] S. Sahoo, Y.K. Ho, Photoionization of Li and Na in Debye plasma environments, Phys. Plasmas 13 (2006) 063301.
[56] S. Kang, J. He, N. Xu, C.Y. Chen, Polarizabilities and hyperpolarizabilities for lithium atoms in Debye plasmas, Commun. Theor. Phys. 62 (2014) 881.
[57] H.W. Li, S. Kar, P. Jiang, Calculations of dynamic dipole polarizabilities of Li and Na atoms in debye plasma using the model potential technique, Int. J. Quantum Chem. 113 (2013) 1493.
[58] H. Li, S. Kar, Polarizabilities of Li and Na in Debye plasmas, Phys. Plasmas (1994-present) 19 (2012) 073303.
[59] Y.Y. Qi, J.G. Wang, R.K. Janev, Static dipole polarizability of hydrogenlike ions in Debye plasmas, Phys. Rev. A 80 (2009) 032502.
[60] H. Lai, Y. Lin, C. Lin, Y. Ho, Bound-state energies, oscillator strengths, and multipole polarizabilities for the hydrogen atom with exponential-cosine screened coulomb potentials, Chin. J. Phys. 51 (2013) 73.
[61] Z. Jiang, S. Kar, Y. Ho, Polarizabilities of two-electron positive ions with screened Coulomb potentials, Phys. Rev. A 84 (2011) 012504.
[62] S. Kar, Y. Ho, Multipole polarizabilities of helium and the hydrogen negative ion with Coulomb and screened Coulomb potentials, Phys. Rev. A 80 (2009) 062511.
[63] L.N. Ning, Y.Y. Qi, Static electric dipole polarizability of lithium atoms in Debye plasmas, Chin. Phys. B 21 (2012) 123201.
[64] S. Kar, H.W. Li, Z.C. Shen, Dynamic multipole polarizabilities of Li and Na atoms interacting with Debye potentials, Open Phys. 11 (2013) 915.
[65] A.N. Sil, S. Canuto, P.K. Mukherjee, Spectroscopy of confined atomic systems: Effect of plasma, Adv. Quantum Chem. 58 (2009) 115.
[66] Q.Y. Ding, S.B. Zhang, J.G. Wang, Simulation of hydrogen emission spectrum in Debye plasmas, Chin. Phys. Lett. 28 (2011) 053202.
[67] Y.C. Lin, C.Y. Lin, Y.K. Ho, Spectral/structural data of helium atoms with exponential-cosine-screened coulomb potentials, Int. J. Quantum Chem. 115 (2015) 830.
[68] Y.C. Lin, C.Y. Lin, Y.K. Ho, Spectral data of helium atoms with screened Coulomb potentials using the B-spline approach, Phys. Rev. A 85 (2012) 042516.
[69] L.Y. Xie, J.G. Wang, R.K. Janev, Y.Z. Qu, C.Z. Dong, Energy levels and multipole transition properties of C^{4+} ion in Debye plasmas, Euro. Phys. J. D. 66 (2012) 1.
[70] Y.Y. Qi, J.G. Wang, R.K. Janev, Bound-bound transitions in hydrogenlike ions in Debye plasmas, Phys. Rev. A 78 (2008) 062511.
[71] T.N. Chang, T.K. Fang, X. Gao, Redshift of the Lyman-alpha emission line of H-like ions in a plasma environment, Phys. Rev. A 91 (2015) 063422.
[72] F.E. Hohne, R. Zimmermann, Oscillator strengths in dense hydrogen plasma-no 'transparency window', J. Phys. B 15 (1982) 2551.
[73] J.C. Weisheit, B.W. Shore, Plasma-screening effects upon atomic hydrogen photoabsorption, Astrophys J. 194 (1974) 519.
[74] Y.Y. Qi, Y. Wu, J.G. Wang, Y.Z. Qu, The generalized oscillator strengths of hydrogenlike ions in Debye plasmas, Phys. Plasmas 16 (2009) 023502.
[75] O. Hiroshi, S. Tokuei, Y. Kaoru, H.F.D. Geerd, Electronic structure of atoms in laser plasmas: A Debye shielding approach, J. Phys. B 38 (2005) 917.
[76] D. Ray, P. Mukherjee, Ionic transitions and oscillator strengths in Debye plasma-A case study, Eur. Phys. J. D-Atomic, Mol. Opt. Plasma Phys. 2 (1998) 89.
[77] B. Saha, P. Mukherjee, G. Diercksen, Energy levels and structural properties of compressed hydrogen atom under Debye screening, Astron. Astrophys. 396 (2002) 337.
[78] S. Kar, Y. Ho, Oscillator strengths and polarizabilities of the hot-dense plasma-embedded helium atom, J. Quant. Spectrosc. Radiat. Transf. 109 (2008) 445.
[79] K.M. Roussel, R.F. O'Connell, Variational solution of Schrodinger's equation for the static screened Coulomb potential, Phys. Rev. A 9 (1974) 52.
[80] H.A. Bethe, E.E. Salpeter, Quantum Mechanics of One- and Two-electron Atoms, Springer Science & Business Media, 2012.
[81] B.W. Shore, On the threshold behaviour of bound-bound and bound-free photoabsorption for the screened Coulomb potentials, J. Phys. B 8 (1975) 2023.
[82] Y.D. Jung, Plasma screening effects on photoionizations in weakly coupled plasmas, Phys. Plasmas 5 (1998) 3781.
[83] L. Zhao, Y. Ho, Influence of plasma environments on photoionization of atoms, Phys. Plasmas 11 (2004) 1695.
[84] S. Sahoo, Y. Ho, On the appearance of a cooper minimum in the photoionization cross sections of the plasma-embedded Li atom, Phys. Res. Int. (2009), 2009.
[85] S. Sahoo, Y. Ho, Photoionization of the excited He atom in Debye plasmas, J. Quant. Spectrosc. Radiat. Transf. 111 (2010) 52.
[86] C. Lin, Y. Ho, Cooper-type minima in quadrupole photoionization of plasma-embedded hydrogen atoms, Phys. Scr (2011) 014051, 2011.
[87] C. Lin, Y. Ho, Influence of Debye plasmas on photoionization of Li-like ions: emergence of Cooper minima, Phys. Rev. A 81 (2010) 033405.
[88] C. Lin, Y. Ho, Quadrupole photoionization of hydrogen atoms in Debye plasmas, Phys. Plasmas 17 (2010) 093302.
[89] T.N. Chang, T.K. Fang, Y.K. Ho, One- and two-photon ionization of hydrogen atom embedded in Debye plasmas, Phys. Plasmas 20 (2013) 092110.
[90] Y.Y. Qi, J.G. Wang, R.K. Janev, Multiple series of shape resonances and near-zero-energy cross section enhancements in photoionization of hydrogen-like ions with screened Coulomb interaction, Euro. Phys. J. D. 63 (2011) 327.
[91] H. Friedrich, Theoretical Atomic Physics, vol. 3, Springer, 2006.
[92] J.W. Cooper, Photoionization from outer atomic subshells. A model study, Phys. Rev. 128 (1962) 681.
[93] J.W. Cooper, Interaction of maxima in the absorption of soft X-rays, Phys. Rev. Lett. 13 (1964) 762.
[94] J.-P. Connerade, Highly Excited Atoms, vol. 9, Cambridge University Press, 1998.
[95] G.J. Hatton, N.F. Lane, J.C. Weisheit, Inelastic electron-ion scattering in a dense plasma, J. Phys. B 14 (1981) 4879.
[96] T. Bornath, M. Schlanges, Ionization and recombination of excited atomic states in a dense nonideal hydrogen plasma, Phys. A Stat. Mech. Appl. 196 (1993) 427.
[97] M. Schlanges, T. Bornath, Ionization and recombination coefficients for a dense nonideal hydrogen plasma: Effects of screening and degeneracy, Phys. A Stat. Mech. Appl. 192 (1993) 262.
[98] Y.D. Jung, Plasma-screening effects on the electron-impact excitation of hydrogenic ions in dense plasmas, Phys. Fluids B 5 (1993) 3432.
[99] Y.D. Jung, Semiclassical transition probabilities for the electron-impact excitation of hydrogenic ions in dense plasmas, Phys. Plasmas 2 (1995) 332.
[100] Y.D. Jung, J.S. Yoon, Plasma-screening effects on semiclassical ionization probabilities for the electron-impact ionization of hydrogenic ions in dense plasmas, J. Phys. B 29 (1996) 3549.
[101] Y.D. Jung, Dynamic plasma screening effects on semiclassical inelastic electron—ion collisions in dense plasmas, Phys. Plasmas 4 (1997) 21.
[102] M.Y. Song, Y.D. Jung, Screening and collective effects on electron-impact excitation of hydrogen-like ions in nonideal plasmas, J. Phys. B 36 (2003) 2119.
[103] K.A. Berrington, W.B. Eissner, P.H. Norrington, RMATRX1: Belfast atomic R-matrix codes, Comput. Phys. Commun. 92 (1995) 290.
[104] P. Burke, C. Noble, V. Burke, R-matrix theory of atomic, molecular and optical processes, Adv. At. Mol. Opt. Phys. 54 (2007) 237.
[105] M.C. Zammit, D.V. Fursa, I. Bray, Electron scattering in a helium Debye plasma, Chem. Phys. 398 (2012) 214.
[106] M.C. Zammit, D.V. Fursa, I. Bray, R.K. Janev, Electron-helium scattering in Debye plasmas, Phys. Rev. A 84 (2011) 052705.
[107] M.C. Zammit, D.V. Fursa, I. Bray, Convergent-close-coupling calculations for excitation and ionization processes of electron-hydrogen collisions in Debye plasmas, Phys. Rev. A 82 (2010) 052705.
[108] I. Bray, A.T. Stelbovics, Explicit demonstration of the convergence of the close-coupling method for a Coulomb three-body problem, Phys. Rev. Lett. 69 (1992) 53.

[109] A. Collaboration, M. Amoretti, C. Amsler, G. Bonomi, A. Bouchta, et al., Positron plasma Diagnostics and temperature control for antihydrogen production, Phys. Rev. Lett. 91 (2003) 055001.
[110] M. Leventhal, C.J. MacCallum, S.D. Barthelmy, N. Gehrelst, B.J. Teegarden, et al., Reappearance of the annihilation line source at the Galactic Centre, Nature 339 (1989) 36.
[111] E.L. Chupp, D.J. Forrest, P.R. Higbie, A.N. Suri, C. Tsai, et al., Solar gamma ray lines observed during the solar activity of August 2 to August 11, 1972, Nature 241 (1973) 333.
[112] G. Weidenspointner, G. Skinner, P. Jean, J. Knodlseder, P. von Ballmoos, et al., An asymmetric distribution of positrons in the Galactic disk revealed by γ-rays, Nature 451 (2008) 159.
[113] H. Schut, A. van Veen, S.W.H. Eijt, R. Job, A.G. Ulyasin, et al., Positron beam and Raman analysis of hydrogen plasma treated and annealed Cz-Si, Nucl. Instrum. Methods Phys. Res. B 186 (2002) 94.
[114] J. Lauwaert, J. De Baerdemaeker, C. Dauwe, P. Clauws, Infrared absorption and slow positron investigation of hydrogen plasma induced platelets in crystalline germanium, J. Mater. Sci. Mater. Electron 18 (2007) 793.
[115] P. Asoka-Kumar, H.J. Stein, K.G. Lynn, Detection of hydrogen-plasma-induced defects in Si by positron annihilation, Appl. Phys. Lett. 64 (1994) 1684.
[116] S.B. Zhang, Y.Y. Qi, Y.Z. Qu, X.J. Chen, J.G. Wang, Positron-impact excitation of hydrogen atoms in Debye plasmas, Chin, Phys. Lett. 27 (2010) 013401.
[117] P. Rej, A. Ghoshal, Positron impact excitations of hydrogen atom embedded in weakly coupled plasmas: Formation of Rydberg atoms, Phys. Plasmas 21 (2014) 093507.
[118] S. Nayek, A. Ghoshal, ns $\rightarrow$ n's transition of hydrogen atom by positron impact with screened Coulomb interactions, Euro. Phys. J. D. 64 (2011) 257.
[119] P. Rej, A. Ghoshal, Positron impact excitations of hydrogen atom embedded in dense quantum plasmas: formation of Rydberg atoms, Phys. Plasmas 21 (2014) 113509.
[120] A. Ghoshal, M.Z.M. Kamali, K. Ratnavelu, Positron scattering from hydrogen atom embedded in weakly coupled plasma, Phys. Plasmas 20 (2013) 013506.
[121] A. Bhattacharya, M.Z.M. Kamali, A. Ghoshal, K. Ratnavelu, Positron scattering from hydrogen atom embedded in dense quantum plasma, Phys. Plasmas 20 (2013) 083514.
[122] S. Nayek, A. Ghoshal, Dynamics of positronium formation in positron-hydrogen collisions embedded in weakly coupled plasmas, Phys. Plasmas 19 (2012) 113501.
[123] J. Ma, Y. Cheng, Y.C. Wang, Y. Zhou, Positronium formation in positron-hydrogen collisions with Debye potentials, Phys. Plasmas 19 (2012) 063303.
[124] S. Sen, P. Mandal, P.K. Mukherjee, Positronium formation in Debye plasma, Euro. Phys. J. D. 62 (2011) 379.
[125] Y. Zhou, K. Ratnavelu, I.E. McCarthy, Momentum-space coupled-channel optical method for positron-hydrogen scattering, Phys. Rev. A 71 (2005) 042703.
[126] M.K. Pandey, Y.C. Lin, Y.K. Ho, Positronium formation in collisions between positrons and alkali-metal atoms (Li, Na, K, Rb and Cs) in Debye plasma environments, J. Phys. B 49 (2016) 034007.
[127] C.G. Kim, Y.D. Jung, Semiclassical electron capture probabilities for proton-hydrogenic ion collisions in dense plasmas, Phys. Plasmas 5 (1998) 2806.
[128] Y.D. Jung, Plasma screening effects on resonant charge transfer in strongly coupled plasmas, Europhys. Lett. 69 (2005) 753.
[129] H. Zhang, J.G. Wang, B. He, Y.B. Qiu, R.K. Janev, Charge exchange and ionization in hydrogen atom-fully stripped ion collisions in Debye plasmas, Phys. Plasmas 14 (2007).
[130] S.L. Zeng, L. Liu, J.G. Wang, R.K. Janev, Atomic collisions with screened Coulomb interactions: excitation and electron capture in H^{+}+H collisions, J. Phys. B 41 (2008).
[131] L. Liu, J.G. Wang, Dynamics of the $H^{+}+H^{-}$ electron capture process in Debye plasmas, J. Phys. B 41 (2008) 155701.
[132] L. Liu, J.G. Wang, R.K. Janev, Dynamics of He^{2+}+H(1s) ionization with screened Coulomb interactions, Phys. Rev. A 77 (2008) 042712.
[133] L. Liu, J.G. Wang, R.K. Janev, Dynamics of He^{2+}+H(1s) excitation and electron-capture processes in Debye plasmas, Phys. Rev. A 77 (2008) 032709.
[134] L. Liu, J.G. Wang, R.K. Janev, Dynamics of $He^{2+}+He^{+}$(1s) and $He^{2+}+He^{+}$(2s) excitation and electron-capture processes with screened Coulomb interaction, J. Phys. B 42 (2009).
[135] D. Jakimovski, L. Liu, J.G. Wang, R.K. Janev, Electron capture in C^{6+}+H collisions in Debye plasmas, J. Phys. B 43 (2010).
[136] Y.Q. Zhao, L. Liu, J.G. Wang, R.K. Janev, P. Xue, Dynamics of O^{6+}+ H electron capture in Debye plasmas and properties of resulting O^{5+}(nl) emission spectra, Phys. Rev. A 82 (2010) 022701.
[137] L. Liu, J. Wang, Dynamics of N^{5+}-H electron capture in Debye plasmas, Matter Radiat. Extrem. 1 (2016) 114.
[138] L. Liu, J.G. Wang, R.K. Janev, Dynamics of O^{8+}+H electron capture in Debye plasmas, Phys. Rev. A 79 (2009) 052702.
[139] W. Fritsch, C.D. Lin, The semiclassical close-coupling description of atomic collisions: recent developments and results, Phys. Rep. 202 (1991) 1.
[140] Y. Wu, J.G. Wang, P.S. Krstic, R.K. Janev, Oscillation structures in elastic and electron capture cross sections for H^{+}-H collisions in Debye plasmas, J. Phys. B 43 (2010) 201003.
[141] Y. Zhang, C.H. Liu, Y. Wu, J.G. Wang, Y.Z. Qu, et al., Low-energy charge transfer in collisions of He^{2+} with H in a Debye plasma, Phys. Rev. A 82 (2010) 052706.
[142] B. Zygelman, D.L. Cooper, M.J. Ford, A. Dalgarno, J. Gerratt, et al., Charge transfer of N^{4+} with atomic hydrogen, Phys. Rev. A 46 (1992) 3846.
[143] M. Pandey, Y.C. Lin, Y. Ho, Investigation of charge transfer and ionization in He-like systems (Li^{+}, Be^{2+}, B^{3+}, C^{4+}, N^{5+}, O^{6+})-hydrogen atom collisions in Debye plasmas, Phys. Plasmas 20 (2013) 022104.
[144] M. Pandey, Y.C. Lin, Y. Ho, Cross sections of charge exchange and ionization in O^{8+}+ H collision in Debye plasmas, Phys. Plasmas 19 (2012) 062104.
[145] A. Bhattacharya, M.Z.M. Kamali, A. Ghoshal, K. Ratnavelu, Charge transfer in proton-hydrogen collisions under Debye plasma, Phys. Plasmas 22 (2015) 023512.